UNIVERSITY *of* York

This is a repository copy of *A model for quantifying the effectiveness of leaky barriers as a flood mitigation intervention in an agricultural landscape*.

White Rose Research Online URL for this paper:
https://eprints.whiterose.ac.uk/id/eprint/207255/

Version: Published Version

Article:

White Rose
university consortium
Universities of Leeds, Sheffield & York

eprints@whiterose.ac.uk
https://eprints.whiterose.ac.uk/

WILEY

A model for quantifying the effectiveness of leaky barriers as a flood mitigation intervention in an agricultural landscape

Martha L. Villamizar[1] [iD] | Chris Stoate[2] | Jeremy Biggs[3] | John Szczur[2] |
Penny Williams[3] | Colin D. Brown[1]

[1]Department of Environment & Geography, University of York, York, UK

[2]The Game & Wildlife Conservation Trust, Allerton Project, Loddington, UK

[3]Freshwater Habitats Trust, Headington, Oxford, UK

Correspondence
Martha L. Villamizar, Department of Environment & Geography, University of York, Heslington, York, YO10 5NG, UK.
Email: martha.villamizarvelez@york.ac.uk

Funding information
Environment Agency; North Anglian RFCC, Grant/Award Number: PGW048

Abstract

Leaky barriers have become an important mitigation option within natural flood management to reduce downstream flood risk. Modelling is a key tool to aid in the design of leaky barrier installations for flood mitigation, but there is limited evidence about the accuracy of model representations of the system. Here, the hydrological model SWAT was combined with a water routing model that simulates multiple leaky barriers as permeable sluice gates. Storage behind individual barriers was quantified using barrier dimensions and LIDAR topography. The model was applied to a series of 27 leaky barriers installed as part of a long-term manipulation experiment into a 11-km^2 intensive lowland agricultural catchment in Leicestershire, England. Evaluation of the model against flow data collected before and after leaky barrier installation and time-lapse photography taken across storm events at individual barriers demonstrated robust model performance (Nash-Sutcliffe efficiency and R^2 across 19 validation events were 0.84 ± 0.14 and 0.91 ± 0.08, respectively). Empirical and modelling data were then combined to demonstrate that the 17,700 m^3 of water storage provided by the 27 leaky barriers reduced peak flows at the catchment outlet by 22 ± 6% and delayed the peak in flow by up to 5 h for 11 storm events recorded after all barriers had been installed. The volume of storage utilised prior to the flood event was a key factor influencing the reduction in peak flow, and a sensitivity analysis indicated that barriers should be permeable to accelerate drain-down of the barrier and help to mitigate risk from multiple storm events occurring in sequence.

KEYWORDS
headwaters, hydrological model, model validation, natural flood management

1 | INTRODUCTION

Projected climate change over the next century is expected to increase the frequency and severity of floods in many locations around the world (Kendon et al., 2014; Murphy et al., 2009). There is an increasing consensus that traditional flood defence engineering approaches to flood alleviation would benefit from working alongside natural processes of water storage and retention moving towards a more sustainable and holistic catchment flood management (Pitt, 2008; Wingfield et al., 2019). In the United Kingdom, the use of natural flood management (NFM) has been incentivised under current environmental stewardship grants across England and Wales

(DEFRA, 2020). NFM involves working with natural hydrological processes to manage sources and pathways of flood waters to enhance the capacity of catchments to store, convey and attenuate flood water (SEPA, 2015; SNIFFER, 2011). Leaky wood barriers installed into flowing water channels are a common NFM intervention that aim to reduce downstream flood risk by temporarily storing flood water and slowing flows by increasing hydraulic roughness (Metcalfe et al., 2017; Wilkinson et al., 2019). Leaky barriers are designed to mimic natural barriers of large woody debris, such as those formed by trees falling into streams (Thomas & Nisbet, 2012; Wohl, 2013). They allow low flows to pass under or through the obstacle but hold back high flows by reducing flow velocity and providing temporary water storage or diverting water onto floodplains.

Empirical investigations and modelling studies on the effectiveness of leaky barriers have mainly studied the impact on peak flow attenuation and delay of single peak flow events but generally they did not consider assessing the impact over multiple events across a long time period. Wenzel et al. (2014) studied the impact of nine large woody debris dams on artificial flood waves with a return period of 3.5 years in a 282-m long river stretch. Results showed a delay of 166 s on peak flow at the reach outlet compared with conditions without barriers, but only a small attenuation of peak discharge (2.2%) was observed. Similarly, Thomas and Nisbet (2012) estimated a 2–3 min delay per large woody debris barrier, but very little effect on the height of the flood peak using field data and modelling for a 1% AEP (annual exceedance probability) flood event in a 9.2-km^2 catchment in the River Fenni in South Wales. Metcalfe et al. (2017) used modelling to demonstrate the large number of leaky barriers needed to generate a significant reduction in peak flow at the catchment level. Their model predicted an 11% reduction in peak discharge using 59 leaky barriers for a 29-km^2 catchment in North Yorkshire. The authors concluded that leaky barriers may reduce flooding during moderate events, but they might be inadequate to prevent flooding from consecutive storm events as storage capacity can be fully utilised by the first storm in the sequence.

Hydraulic modelling studies have considered leaky barriers as sluice gates (Metcalfe et al., 2017) or as a combination of a sluice gate and a weir (Leakey et al., 2020). Metcalfe et al. (2017) combined TOP-MODEL with hydraulic equations for trash screen structures and sluice gates to model leaky barriers. However, the riverbank and channel were simulated using a regular trapezoidal shape with uniform measurements along the river network that ignored the variable morphology of the channel. Leakey et al. (2020) studied leaky barriers in the laboratory as a combined sluice gate with weir overflow, but using smooth vertical screens instead of real wood logs which did not include the natural permeability and friction of leaky barriers. These studies simulated individual peak flow events which is a common approach in hydraulic modelling; however, to assume that the additional storage created behind a leaky barrier is always empty before a peak flow event will likely overestimate the impact on peak flow reduction.

Few studies have been able to test the accuracy of the physical representation of leaky barriers (Addy & Wilkinson, 2019) and as yet,

there is no agreed way of representing leaky barriers in models (Addy & Wilkinson, 2019; Burgess-Gamble et al., 2018). The simplest method to quantify the effect of leaky barriers is by studying the relative difference between flood events pre- and post-installation of NFM measures. For example, modelling for Pickering, the United Kingdom did not seek to simulate individual barriers, but rather the impact of NFM was studied by comparing simulated flow and water levels from a 2D hydraulic model set-up for pre-NFM conditions to observations made in the catchment during flood events in 2015 (Forest Research, 2016). Nevertheless, a validated model that describes the hydrodynamics of individual leaky barriers would be a more useful method for flood planning.

This study proposes a physically based model that represents multiple leaky barriers within a catchment using field measurements of leaky barriers and channel profiles as well as improved LIDAR topography data. The model is developed for the Eye Brook catchment which is part of a long-term manipulation experiment sited in an intensive lowland agricultural landscape in the English midlands (Williams et al., 2020). Model hydrology is first validated for large storm events occurring before the installation of NFM, and then the leaky barriers component is validated for storm flows modified by NFM. The model is then applied to assess the impact of leaky barriers in delaying and reducing peak flow across a large number of storm events and to investigate key design features for the barriers.

2 | METHODOLOGY

2.1 | Study area

The study catchment is the headwater of the Eye Brook (Leicestershire) with an area of 10.9 km^2, with the Eye Brook being one of 15 tributaries of the River Welland (Figure 1a). Soils in the catchment are mainly heavy clays (Ragdale and Denchworth association; Figure 1b) which are normally tile-drained under agricultural land uses (Cranfield University, 2014). The land cover is mainly pasture (51%) and arable farmland (36%) (Figure 1c) (Rowland et al., 2017); small areas of a mixture of broadleaf and coniferous woodland cover about 9% of the land area; and urban and suburban land accounts for 4% of the catchment. Slopes in the catchment are generally steep (81% of the catchment area is steeper than 4°) and altitude ranges between 131 and 221 m above sea level (Figure 1d).

Since 2012, water level has been monitored every 15 min at the headwater catchment outlet (NGR: SK763029) and then converted into stream flow (m^3 s^{-1}) using a site-specific rating curve (NSE = 0.69, R^2 = 0.86 and PBIAS = −2). Weather data at 30-min resolution were recorded by a COSMOS-UK (Fry et al., 2014) meteorological station at Loddington (NGR: SK796020, 142 m a.s.l), located 3.5 km outside of the study catchment. Weather data at hourly resolution from a meteorological station at Skeffington (SK74425, 201 m a.s.l) (Meteoblue, 2018) were used to fill gaps on dates when weather data were missing from COSMOS-UK.
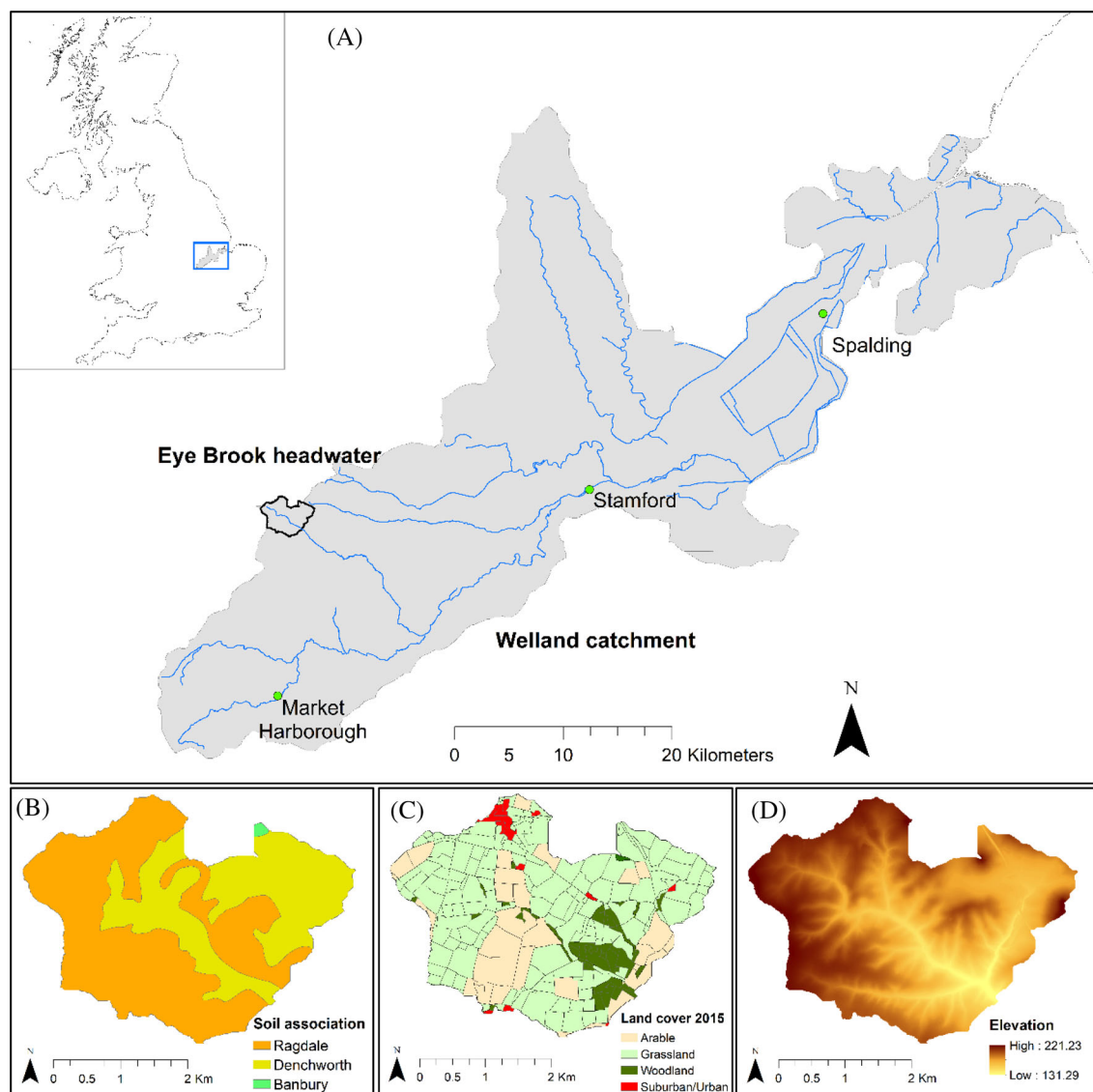
FIGURE 1   Maps of (a) the Welland catchment showing the location of the headwater of the Eye Brook and (b) soils, (c) land use and (d) elevation in the Eye Brook headwater catchment. [Color figure can be viewed at wileyonlinelibrary.com]

2.2 | Natural flood management interventions: Leaky barriers

Leaky barriers were selected as a suitable flood reduction measure following consultation with local landowners who stipulated that water storage should be retained in-channel and on adjacent non-cropped riparian zones where present. A synchronisation analysis for the wider Eye Brook catchment showed that the three main stream reaches in the headwater catchment were the only tributaries suitable for NFM whereby measures would desynchronise flow and reduce downstream flood risk (SI Section A1.1 and A2.1). A total of 27 leaky barriers were installed in the headwater catchment between 2016 and 2018 (Figure 2). Installation dates and total capacity were barriers 1–7, September 2016, 887 m³; barriers 8–18, September 2017, 8090 m³; and barriers 19–27, September 2018, 8697 m³. Leaky barriers were built from 3 m lengths of ash and sycamore tree trunks of 10–20 cm

diameter obtained from the local area where possible. Wooden trunks of the biggest leaky barriers, particularly on the main channel, were wired together and secured using anchor wood poles. The design included a gap at the base between 9 and 78 cm from the stream bed to allow free movement of water during normal flow conditions. Barrier heights were between 1.2 and 2.5 m from the stream bed to retain water during high flow events. Figure A1 shows photographs of some of the barriers, and video A1 shows time-lapse photographs for leaky barrier 8 for a peak flow event on March 12th 2019.

2.3 | Modelling the effect of leaky barriers on streamflow

Modelling work combined the hydrological model SWAT to simulate the flow of water entering the stream network and a water routing

FIGURE 2 Location of 27 leaky barriers built in the headwater catchment of the Eye Brook. [Color figure can be viewed at wileyonlinelibrary.com]

model using the Muskingum approach (McCarthy, 1938) to route streamflow to the outlet of the headwater catchment and incorporate the effect of leaky barriers.

2.3.1 | SWAT

The Soil and Water Assessment Tool (Arnold et al., 1998) was used to simulate stream flow in the Eye Brook catchment. SWAT is a physically based hydrological model, designed to estimate impacts of land management practices in complex watersheds. Hydrological response units (HRUs) in SWAT are defined as areas of land with the same soil, land use and slope that are assumed to behave similarly in the model. The hydrological routines within SWAT operate at a sub-daily timestep and account for precipitation, evaporation, infiltration (Green & Ampt, 1911), plant uptake, overland flow, sublateral flow, drain flow, percolation, channel transmission losses, channel routing and shallow aquifer and deep aquifer recharge. Overland flow occurs when rainfall intensity exceeds the soil infiltration rate. Tile drainage occurs when the water table extends above drain depth (Neitsch et al., 2011).

The headwater catchment was delineated in ArcSWAT using a map of soil associations for the study area (Cranfield University, 2014) (Figure 1b), a land cover map (LCM 2015 CEH) (Rowland et al., 2017) (Figure 1c) and a LIDAR 2-m digital elevation model (DEM)

(Environment Agency, 2015) (Figure 1d). Spatial slope data were classified into four ranges in the model (0–4%, 4–8%, 8–12% and >12%). The catchment was finally defined by seven sub-catchments and 179 HRUs. Tile drains were simulated for all arable land located on clay soils. Cropping varied according to the actual rotations recorded for the catchment. A simulation at hourly resolution (using SWAT revision 650) for the period 2016–2019 was obtained using calibrated parameters at a daily time step (Table A1). The first year was used as warm up period in the model.

2.3.2 | Modelling of leaky barriers

The maximum storage of individual leaky barriers located in the headwater catchment (Figure 2) was calculated using a LIDAR 1-m DEM, and the dimensions of each leaky barrier. Field measurements of channel profiles for stream reaches where leaky barriers had been installed were taken to validate and correct the DEM to minimise errors due to limitations in its spatial resolution and issues with LIDAR's penetration capabilities through water and vegetation. A vertical correction factor was derived and applied to a buffer width along the river line by comparing measured channel profiles with interpolated elevation data at measured cross sections taken from LIDAR that was flown over the catchment area in November 2013 (Environment Agency, 2015).

The spatial analysis to estimate the maximum storage capacity of each barrier consisted in the spatial intersection of a polygon with the DEM at the barrier location and positioned offset at the height of the barrier using ArcGIS 10.4. The surface difference between the two spatial layers was used to generate the maximum storage volume and inundated surface area for each barrier. A total storage of 17,674 m^3 was estimated for the 27 barriers installed in the headwater catchment (range 30 to 2221 m^3 per barrier including both stream channel and floodplain storage).

Upstream water flow and depth for each barrier were generated using hourly simulated flow within each reach of the stream network from SWAT, draining areas to each barrier and cross-sectional areas at the barrier locations. The hydrodynamics of leaky barriers were simulated as permeable sluice gates (Figure 3). The downstream flow for each barrier was simulated according to hourly water level estimates (h_1), the barrier height at maximum storage (h_{max}) and the gap at the base of each barrier (a). It was assumed

that water flows freely beneath the barrier when water level is below or equal to the barrier bottom opening ($Q_{in} = Q_{out}$). Leaky barriers will start to store water when the water level exceeds the height of the gap at the bottom of the barrier (a). However, leaky barriers are by definition permeable since water flows continuously beneath the barrier (Q_d) and also through the naturally occurring gaps between logs within the barrier (Q_p). When the maximum storage capacity of the barrier is reached (i.e., water level reaches the barrier height, h_{max}), excess water flow (Q_e) is assumed to flow over the barrier. This approach will under-estimate the storage somewhat because water level will actually rise above the top of the barrier due to frictional forces in the same way as for a weir, but this effect is not considered in the model. Since this is a 1D model, floodplain storage was treated similarly to channel bank storage in terms of downstream routing of water flows, that is, using the same surface roughness and not explicitly simulating the effect of shallow water flow on the floodplain.

FIGURE 3 Sketch showing the leaky barriers modelling approach a) when the water flows freely beneath the barrier; b) when water flows through the barrier at a water level below the top of barrier height; and c) when the water level exceeds the maximum storage capacity of the barrier. Q_{in} is the water inflow; Q_{out} is the water outflow; Q_d is the sluice-gate flow; Q_p is the water that flows through the gaps between logs within the barrier; Q_e is the excess water flow when the water level reaches the barrier maximum storage h_{max}; h_1 is hourly water level; and a is the gap at the base of each barrier. [Color figure can be viewed at wileyonlinelibrary.com]
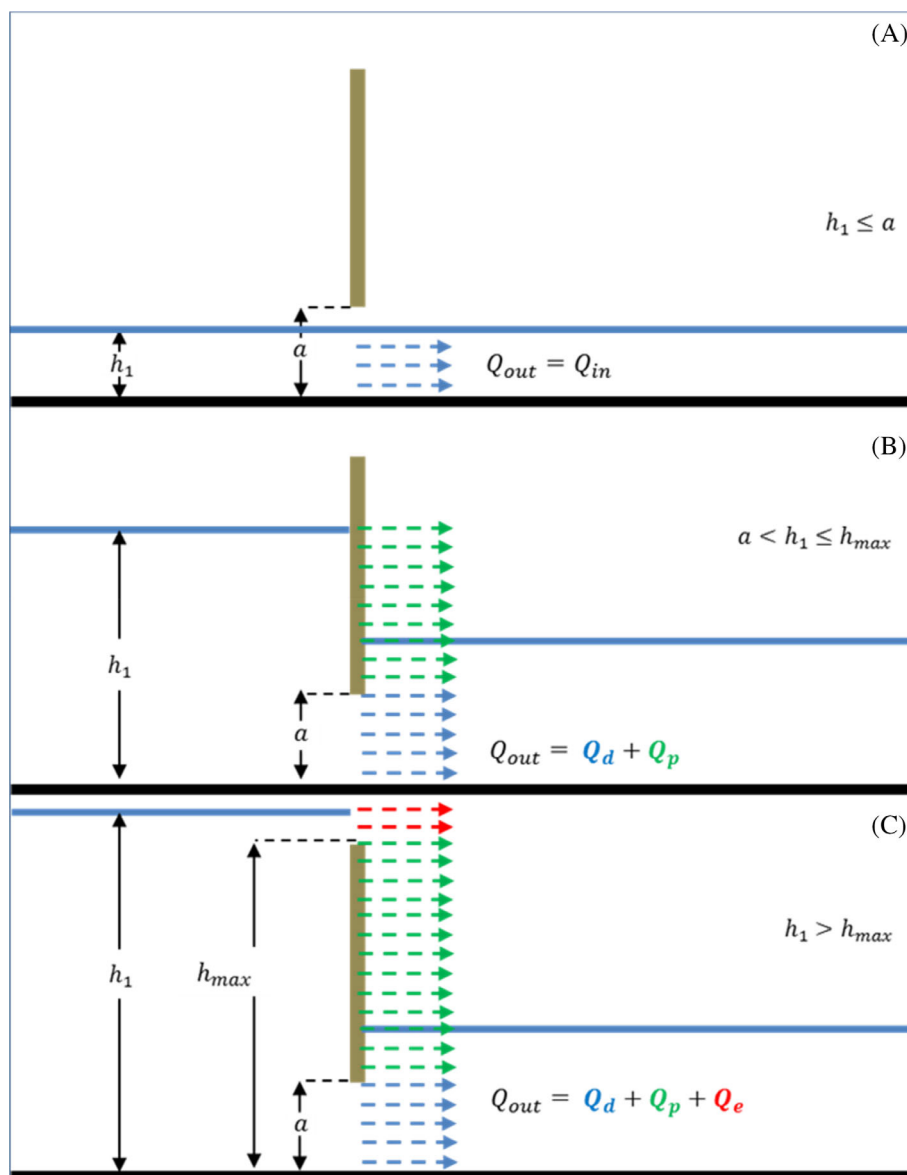
The conventional sluice-gate discharge equation (Swamee, 1992) was used to calculate the barrier discharge rate flowing beneath the barrier, Q_d (m^3 s^{-1}):

$$Q_d = C_d ab \sqrt{2gh_1} \tag{1}$$

where a is the height of the gap from the stream bed (m) to the bottom of the barrier, b is the width at the base of the barrier (m), h_1 is the upstream water depth (m), g is the gravitational acceleration (m s^{-2}) and C_d is the discharge coefficient (−). The typical discharge coefficient is approximately 0.611 for free-flow conditions (Swamee, 1992).

The permeability of the barrier was simulated as a constant factor of the impounded water (Equation 2):

$$Q_p = p\, Q_{\text{imp}} \tag{2}$$

where Q_p is the water that will flow through the gaps between wood logs (m^3 s^{-1}), p is a permeability factor ($0 < p < 1$) and Q_{imp} is the impounded water behind the barrier expressed as a flow ($Q_{in} - Q_{out}$; m^3 s^{-1}).

2.3.3 | Muskingum method for channel routing

The Muskingum method (Equation 3; McCarthy (1938)) was incorporated to route the water downstream and to consider channel storage and roughness. The outflow rate at the end of the time step ($Q_{r\_out_{t2}}$) is calculated as

$$Q_{r\_out_{t2}} = C_0 Q_{r\_in_{t1}} + C_1 Q_{r\_in_{t2}} + C_2 Q_{r\_out_{t1}} \tag{3}$$

where Q_{r_in} and Q_{r_out} are the inflow and outflow from the reach (m^3 s^{-1}), $t1$ and $t2$ denote time at the beginning and end of the time step (s) and the coefficients C_0, C_1 and C_2 (−) are defined as

$$C_0 = \frac{\Delta t + 2K_m x}{\Delta t + 2K_m - 2K_m x} \tag{4}$$

$$C_1 = \frac{\Delta t - 2K_m x}{\Delta t + 2K_m - 2K_m x} \tag{5}$$

$$C_2 = \frac{-\Delta t + 2K_m - 2K_m x}{\Delta t + 2K_m - 2K_m x} \tag{6}$$

with $C_0 + C_1 + C_2 = 1$. K_m is the travel time of the flood wave through the reach (s), and x is a dimensionless weighting coefficient with a value between 0.0 and 0.5 that controls the relative importance of inflow and outflow in determining the storage in a reach. Values of x between 0.0 and 0.3 are recommended for streams with a mean value near 0.2 (Neitsch et al., 2011; Viessman & Lewis, 1996) that was used for all reaches here. K_m can be estimated as (Viessman & Lewis, 1996)

$$K_m = \frac{L}{c} \tag{7}$$

where L is the length of the reach (m) and c is the celerity corresponding to the kinematic wave velocity (m s^{-1}).

Manning's equation for velocity in a triangular channel v was used to calculate the celerity c (Equations 8 and 9):

$$c = \frac{5}{3}v \tag{8}$$

$$v = \frac{Rh^{2/3} s^{1/2}}{n} \tag{9}$$

where v is the average flow velocity (m s^{-1}), Rh is the hydraulic radius of the flow (m), s is the slope of the channel bed (m m^{-1}) and n is Manning's roughness coefficient (−). Rh is calculated as the ratio of the cross-sectional area of the flow and the wetted perimeter of the flow (Neitsch et al., 2011) based on measurements of the channel dimensions of the width top and bottom, flow depth and the slope of the reach. A calibrated Manning's n roughness coefficient of 0.05 was used in the model.

2.3.4 | Permeability of leaky barriers

A sensitivity analysis of the permeability factor, p, in the simulation of peak flow and water storage was carried out using the modelling framework (for all 27 barriers and for a single leaky barrier) and design flood events with a 1-in-2-year and 1-in-10-year return frequency (see SI section A1.2 for details of derivation). Permeability factors between 0 (equivalent to not having any barriers) and 1 (equivalent to an impermeable sluice gate) at increments of 0.1 were tested in the model.

The actual permeability of leaky barriers was studied by placing time-lapse cameras and gauging boards next to seven barriers (8, 11, 12, 14, 15, 18 and 26; Figure 2) to record water depth across peak flow events. The design of barriers was irregular and differed between barriers, so their permeability was difficult to estimate from their geometry. Therefore, recordings of barriers during storm events were used to estimate an average permeability factor by adjusting the factor within the model to obtain the closest match to the observed water depth behaviour. Average permeability across the seven barriers with cameras was 40 ± 15% (Figure A6 and Table A2), and this value was assumed to apply for all barriers within the model.

2.3.5 | Modelling evaluation and statistical analysis

The simulation of stream flow was evaluated using observed flow data from the gauging station at the catchment outlet (calibration period December 2017 to April 2018; validation period March to October 2019). The period 2012–2013 was very wet with larger peak flow events than those recorded in 2016–2019, so additional validation was undertaken against flow recorded in 2012–2013 when no barriers were present in the catchment. Goodness-of-fit statistics including Nash–Sutcliffe model efficiency (NSE; Nash & Sutcliffe, 1970), the

coefficient of determination and percentage bias (PBIAS) were used to evaluate model performance (Section A1.3). Moriasi et al. (2007) published ratings for recommended statistics to assess stream flow simulations from SWAT for monthly time steps. They considered satisfactory model results with NSE values >0.5 and −25 < PBIAS < +25.

A multiple regression analysis was carried out to investigate the explanatory factors for the impact of leaky barriers on reduction in peak flow at the headwater catchment outlet for storm events that occurred between December 2017 and October 2019. A linear regression model was fitted using Excel Data Analysis Toolpack. Factors in the analysis included (i) the simulated peak flow without barriers, (ii) the storage in use before a peak flow event, (iii) the maximum storage used by the peak flow event, (iv) rainfall amount, (v) rainfall duration and (vi) antecedent soil moisture conditions. The statistical significance of the overall fit and individual factors was tested using the coefficient of determination (R^2), residual plots, the significance F (<0.05) of the ANOVA test and the p-values (<0.05) for the coefficients in the regression model.

3 | RESULTS

3.1 | Simulation of stream flow

The coupled model comprising SWAT and the water routing/leaky barrier code gave a satisfactory simulation of streamflow from the headwater catchment (Figure 4). The main divergence was that simulations overpredicted small flow events during low flow periods due to a flashier response to small events in the model compared with the

observed flow and mismatches in the baseflow behaviour. Model calibration in this study was intended to favour the matching of high peak flow events as small events are not important for flood risk assessment and will normally flow freely under leaky barriers. The model accurately simulated the magnitude (minor overestimation by an average of 2.6 ± 8.5%) and timing (average deviation 0 ± 1 h) of peak flows, whereas the recession time from peak was slightly shorter than was actually observed. Peak flow underestimation was obtained for the storm event on 15 October 2019 during the validation period. This was a major peak flow event after 32.6 mm of rainfall over two consecutive days which caused the cascade collapse of four leaky barriers in the main channel (barriers 8, 12, 13 and 14 in Figure 3). Therefore, all water stored by these barriers was released over a short period causing an unusually high signal at the headwater outlet. Assessment of flow forces on large wood in rivers. The lack of records of exact times when each barrier failed made it impossible to simulate this peak.

Goodness-of-fit statistics for individual peak flow events (Table 1) were generally within very good and satisfactory ranges as defined by Moriasi et al., 2007. Nash-Sutcliffe efficiency and R^2 across 19 validation events were 0.84 ± 0.14 and 0.91 ± 0.08, respectively. Average NSE values of 0.85 ± 0.11 and 0.80 ± 0.14 were obtained for peak flow events during the calibration and validation period, respectively. The linear relationship between the observed and the simulated flow was good (R^2 > 0.70), and PBIAS values were within satisfactory ranges (values for individual events were in the range −13.7 to 23.1). The model was tested against. Goodness-of-fit statistics for large events from 2012–2013 before leaky barriers were installed showed similar model performance to that obtained for the calibration and validation periods (Table 1). Figure 5 shows that the model was able to
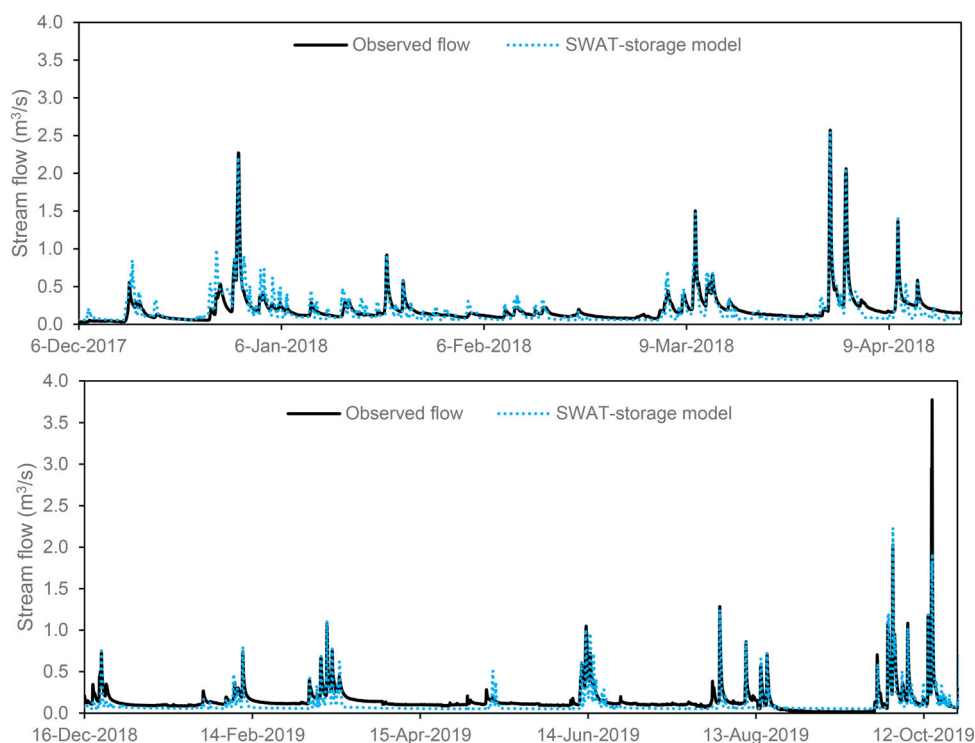

FIGURE 4 Comparison between observed flow and that predicted using SWAT coupled with the water routing model for the calibration period (top; December 2017–April 2018) and validation period (bottom; December–October 2019). [Color figure can be viewed at wileyonlinelibrary.com]

TABLE 1 Goodness-of-fit statistics for flow simulations for the calibration and validation periods.

Number of barriers	Date	Observed peak flow	Simulated peak flow	NSE	R^2	PBIAS	Δt
Calibration period							
21	30/12/2017	2.271	2.215	0.93	0.94	−6.65	0
	22/01/2018	0.917	0.918	0.83	0.92	−5.74	0
	24/01/2018	0.578	0.575	0.75	0.83	−4.58	−1
	10/03/2018	1.504	1.502	0.75	0.82	9.01	1
	31/03/2018	2.574	2.547	0.96	0.98	5.26	0
	02/04/2018	2.061	2.069	0.93	0.96	−13.7	−2
	10/04/2018	1.364	1.437	0.97	0.98	1.52	0
	13/04/2018	0.583	0.578	0.68	0.78	4.14	−1
Validation period							
30	22/12/2018	0.724	0.754	0.73	0.86	8.18	0
	10/02/2019	0.745	0.801	0.75	0.81	9.66	0
	10/03/2019	0.667	0.691	0.94	0.95	2.63	0
	12/03/2019	1.075	1.119	0.83	0.86	4.39	0
	14/03/2019	0.760	0.781	0.59	0.70	0.83	0
	31/07/2019	1.285	1.246	0.96	0.97	5.93	0
	09/08/2019	0.861	0.862	0.84	0.87	2.52	−1
	17/08/2019	0.716	0.731	0.61	0.86	23.1	−1
	30/09/2019	2.027	2.233	0.92	0.96	−3.73	0
	06/10/2019	1.085	1.027	0.98	0.98	−1.04	0
	13/10/2019	1.180	1.189	0.65	0.97	−2.00	1
Post-validation period							
0	21/11/2012	3.036	2.709	0.64	0.78	23.9	0
	20/12/2012	2.498	2.416	0.93	0.97	−14.3	0
	22/12/2012	1.465	1.574	0.90	0.91	−0.44	0
	24/12/2012	2.921	2.974	0.98	0.99	8.54	0
	27/12/2012	2.279	2.243	0.98	0.99	−3.47	0
	27/01/2013	4.691	4.693	0.76	0.85	20.3	−2
	14/02/2013	3.107	3.170	0.99	0.99	7.11	0
	28/10/2013	3.962	4.066	0.95	0.97	6.72	1

Abbreviations: NSE, Nash–Sutcliffe model efficiency; PBIAS, percentage bias; R^2, coefficient of determination; Δt, offset of the simulated peak flow compared with the measured peak flow (Δt = $t_{sim} - t_{obs}$).

match observed flow very closely for the largest storm events during this period.

3.2 | Impact of leaky barriers on peak flow for individual storm events

The model incorporating leaky barriers gave an excellent fit to measured flow at the outlet of the headwater catchment (Figure 6). The figures demonstrate how the model was able to match both the timing and magnitude of peak flows modified by the action of the leaky barriers. Given the strong fit of the model to observed behaviour, the difference between model simulations for a single event with and without leaky barriers incorporated provides a measure of the impact of the barriers in

delaying and reducing peak flows. Thus for example, peak flow was predicted to be delayed by 3 h and reduced by 22% for the relatively small event in July 2019 (Figure 6c), whereas the delay was 5 h and the reduction in flow was 16% for the larger event at the end of September 2019 (Figure 6d). Where multi-peak events occurred, the barriers had a much larger impact on the first peak in flow than on subsequent peaks (Figure 6a,d); flow during the first part of the event filled the storage behind the barrier and there was limited time before the second peak in flow for the release of stored water meaning that there was less storage available to influence that second peak. In addition to reducing peak flow, leaky barriers were predicted to increase the recession time following peak flow as backwater was slowly released (Figure 5). There was good agreement between the rate of recession that was observed in the presence of leaky barriers and that simulated by the model.
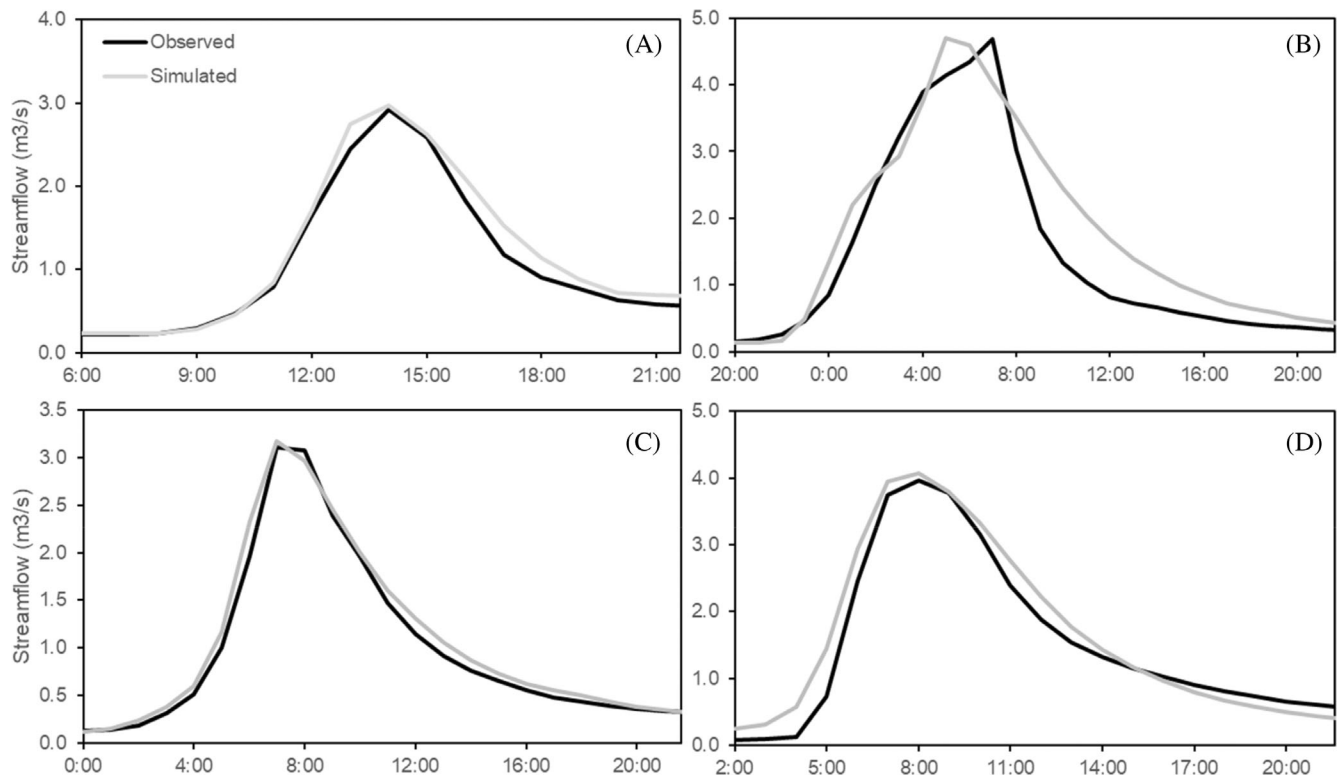
FIGURE 5 Comparison between observed and simulated peak flow events on (a) 24 December 2012; (b) 26–27 January 2013; (c) 14 February 2013 and (d) 28 October 2013, before barriers were installed in the Eye Brook headwater catchment.
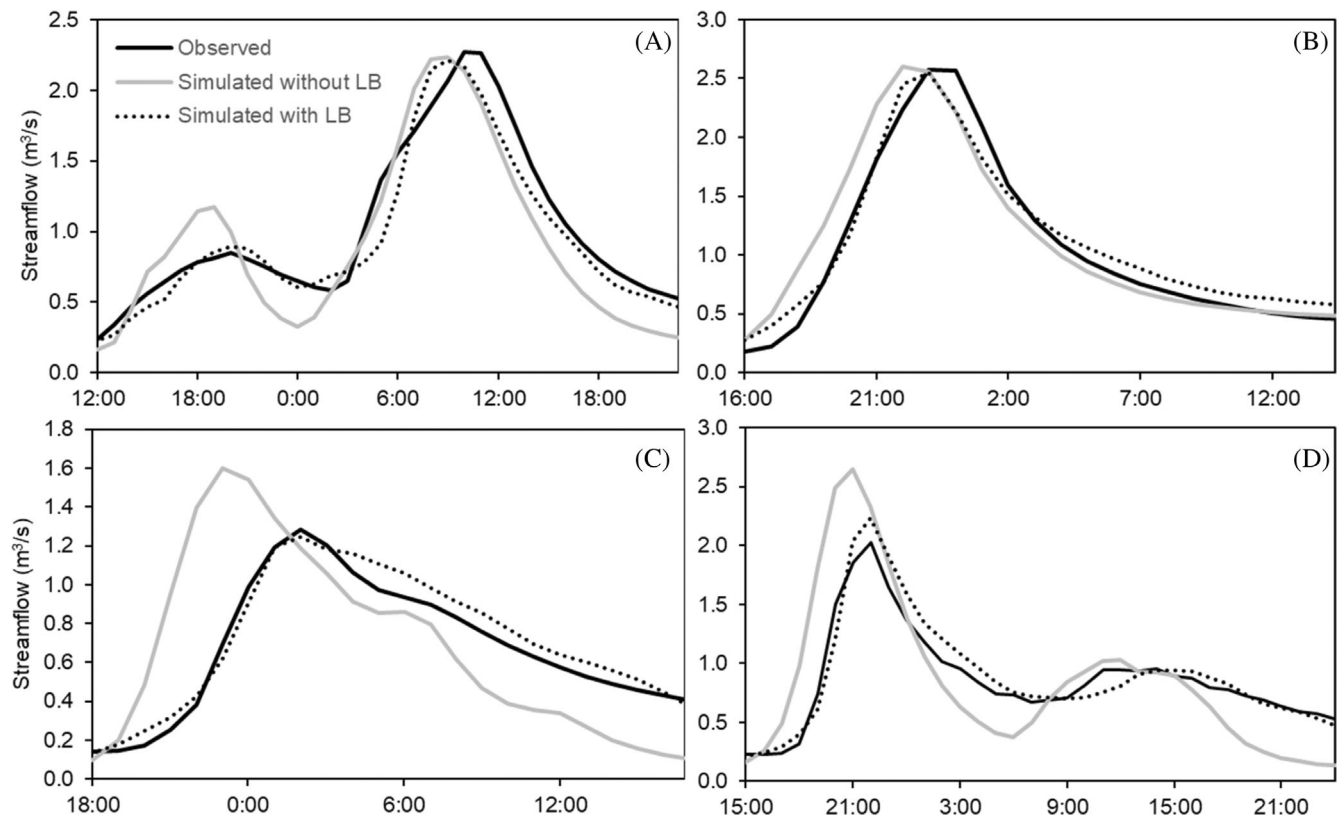

FIGURE 6 Comparison of observed and simulated peak flow events on (a) 29–30 September 2017; (b) 30–31 March 2018; (c) 30–31 July 2019 and (d) 30 September–1 October 2019, after barriers were installed in the Eye Brook headwater catchment. LB = leaky barriers.

Across all of the storm events analysed, modelling results demonstrated a reduction in peak flow from the headwater catchment of up to 51% for individual events during the period 2017–2019 (Table 2). The number of leaky barriers and hence the maximum storage capacity available in the catchment greatly influenced the impact on peak flow reduction. Predicted peak flow reductions for events from December 2018 onwards, when the storage of leaky barriers was nearly doubled, were on average increased by 27% compared with peak flow reductions predicted for events in 2017–2018. The 27 leaky barriers reduced peak flows at the catchment outlet by 22 ± 6% for 11 storm events recorded after all barriers had been installed. In addition, simulated delay in the timing of peaks also increased from 1–3 h in 2017–2018 (with 18 barriers) to up to 5 h in 2018–2019 (with 27 barriers).

A regression analysis (Section A2.2) showed that there was no significant relationship ($p > 0.05$) between the reduction in peak flow across individual events (Table 2) and variables including the size of the peak flow event without barriers, rainfall amount and duration, or antecedent soil moisture conditions. However, the simulated storage in use before the peak flow event occurred and the simulated maximum storage used across the event (primarily determined by event size) explained 44% ($p = 0.034$) and 65% ($p = 0.002$) respectively of the variability in peak flow, and both factors were statistically significant with a negative association as

expected. Interaction effects between both storage factors were not significant ($p > 0.05$). The combined effect of both storage variables explained 77% of the variability in the observed reduction in peak flow from the catchment.

3.3 | Impact of structure permeability and stream morphology on the effectiveness of leaky barriers

The permeability of leaky barriers is an important design feature because it controls the rate at which water backs up behind the barrier as flow increases and the rate at which stored water is released on the falling limb of the hydrograph. The value cannot be determined easily due to the irregular design of leaky barriers. The sensitivity analysis of the permeability factor on the effectiveness of the barriers showed that this parameter was only slightly sensitive for more frequent flood events and nearly insensitive for less frequent flood events (Figure 7; Figures A6 and A7 provide analysis for a single barrier). For instance, the reduction in peak flow from the headwater catchment that was predicted for a 1-in-2-year flood event only varied between 13 and 18%. The very low sensitivity to the permeability factor for the 1-in-10-year event arose because storage was completely filled, and the barrier was over-topped by the time the peak in flow occurred. The typical permeability of the leaky barriers in

TABLE 2 Estimated impact of leaky barriers built in the headwater catchment on peak flow at the headwater outlet during storm events recorded in 2017/18 (barriers partially installed) and 2018/19 (barriers fully installed).

Event date	Simulated peak flow without barriers	Simulated peak flow reduction with barriers	Time delay	Simulated storage in use before peak flow event	Simulated maximum storage used by the peak flow event
	m³ s⁻¹	%	h	% of total storage†	
30/12/2017	2.236	1.0	0	37.4	99.4
22/01/2018	1.551	41	3	0.99	69.6
24/01/2018	1.173	51	0	0.61	67.1
10/03/2018	1.634	8.1	2	57.4	97.6
31/03/2018	2.602	2.1	1	10.8	100
02/04/2018	2.266	8.7	0	1.87	100
10/04/2018	1.621	11	0	21.2	97.1
13/04/2018	0.760	24	0	25.1	55.7
22/12/2018	1.030	27	4	0.86	60.8
10/02/2019	1.005	20	4	1.03	65.5
10/03/2019	0.903	23	4	3.08	58.2
12/03/2019	1.555	28	3	8.21	88.5
14/03/2019	0.869	10	5	0.84	65.6
31/07/2019	1.602	22	3	3.46	87.5
09/08/2019	1.072	20	4	0.51	66.1
17/08/2019	0.929	21	4	2.53	60.6
30/09/2019	2.644	16	5	0.40	49.4
06/10/2019	1.516	32	3	0.69	85.4
13/10/2019	1.625	27	1	0.79	89.8

†Maximum storage capacity changed for events: 8977 m³ until 2018 and 17,674 m³ from 2019.
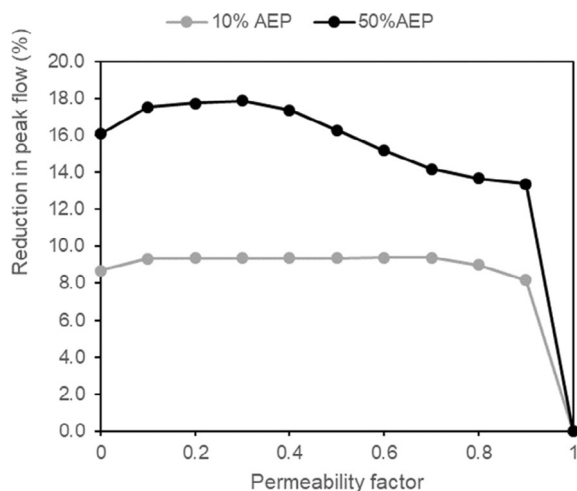
FIGURE 7 Sensitivity analysis showing how reduction in peak flow is predicted to change according to the permeability of the barriers (*p*). The analysis was undertaken for 1-in-2- (50% AEP) and 1-in-10-year flood events (10% AEP) at headwater catchment outlet.

this study was estimated using time-lapse photography to be around 0.4 (Section A2.4).

Scour was observed around the channel bed and bank erosion around some leaky barriers with smaller bottom gaps. Changes in the stream channel around the barriers in the Eye Brook catchment were considered in the model by adjusting the vertical gap at the bottom of the barrier and the barrier height in Equation 1 with data obtained from measurements taken for each leaky barrier two to three years after being built (Table A3). Channel scour was observed at 22 of the 27 leaky barriers, with bed erosion of between 4 and 78 cm depth (average 29 cm). Sediment deposition and debris accumulation in the channel bed was observed at five barriers, with accumulation depths between 2 and 51 cm (average 18 cm).

4 | DISCUSSION

4.1 | Model application, uncertainty and limitations

Modelling studies on the effectiveness of multiple leaky barriers on reducing downstream flood risk across catchments are still limited. An informative model should assess the effect over long timescales and over a wide range of flood magnitudes (Addy & Wilkinson, 2019). The present study presents a modelling approach linking a physically based catchment scale model to a modified Muskingum water routing model that represents leaky barriers as permeable sluice gates. The model was set up to simulate 27 leaky barriers, calibrated and validated for a range of peak flow events over a three-year period. This modelling approach can capture the integrated impact of dynamic utilisation of storage including fill up and drain down of barriers between events which is important for understanding the cumulative flood attenuation effect on downstream flow (Hankin et al., 2020; Muhawenimana et al., 2021). The model will thus have applications in

the design and assessment of the effectiveness of leaky barriers for NFM. Planning the location of barriers in intensively farmed agricultural catchments requires particular care because of the potential to impact negatively on farm businesses. Landowners will generally stipulate that cropland should not be inundated, and logistic accessibility to sites is a further constraint in these intensively managed landscapes.

Different sources of uncertainty have been considered in the model and simulations reported here, including the impact of the permeability factor on backwater storage and peak flow reductions. However, some uncertainties remain including how the model simulates flow where water levels exceed the top of the leaky barriers, consideration of flow interactions between barriers, and lack of explicit consideration of slowing of flow that spills onto the floodplain. Leakey et al. (2020) simulated leaky barriers in the laboratory as a combined sluice gate and rectangular weir. Since there were no data to calculate the hydraulic jump when the maximum storage capacity of the leaky barriers was exceeded, weir discharges and overbank floodplain dynamics were not considered in the model here. In addition, leaky barriers were simulated for free-flow conditions, so any interaction between the downstream water depth and upstream flow was not accounted for in the model. Consideration of submerged conditions in the model is particularly important when leaky barriers are installed close to each other as storage behind a downstream barrier has potential to cause a backwater effect that will modify flow through the upstream barrier (Leakey et al., 2020). Depth loggers upstream and downstream of each barrier would be required to calibrate parameters that estimate the hydraulic jump and submerged state equations of the barriers (Holdhusen et al., 1950; Villemonte, 1947). The model did not include any special treatment of the floodplain in terms of surface roughness or explicitly simulating the effect of shallow water flow. Adding a 2D model to simulate the floodplain may also improve the accuracy of the model.

4.2 | Implications for key design features and stability of leaky barriers

The findings reported here support observations from other studies which show that an extensive series of leaky barriers across upper catchments and tributaries is required to have an impact on downstream flood attenuation and peak flow delay (Bark et al., 2021; Metcalfe et al., 2017; Thomas & Nisbet, 2012). The impact of leaky barriers on peak flow reduction at the headwater catchment outlet increased when the number of barriers, and consequently its associated storage was doubled in 2018 and leaky barriers were installed in all three tributaries of the headwater catchment. Metcalfe et al. (2017) studied the effect of 40, 50 and 59 leaky barriers in a 29 km^2 catchment. Modelling results showed that 40 and 50 barriers were predicted to have only a minor effect on time delay (0 and 0.25 h delay, respectively), and 59 leaky barriers were needed to obtain a substantial effect (>2 h peak flow delay and >10% peak flow reduction). The main reason given was that the storage capacity filled

shortly after the beginning of storm peaks when insufficient barriers were installed. The authors also noticed that barriers still continued to drain after storm events. The increase in recession times that was observed here following installation of NFM quantifies the slow release of water stored behind leaky barriers.

The spatial location and design of leaky barriers influence their effectiveness and stability. The gap at the base of the barriers proved to be particularly important for their design. A vertical gap that is higher than average winter flows allows the barrier to retain water only during the largest flow events and increases storage availability at the time of flood events. The increase in channel erosion due to flow acceleration caused by the presence of the barrier will affect the performance and stability of the barrier in the long term. Other studies observed that the spatial distribution of the shear stress is affected by the presence of leaky barriers in the river channel (Daniels & Rhoads, 2004; Manga & Kirchner, 2000), creating patches of scour around the barrier (Smith et al., 1993) and sediment deposition downstream as a result of reduced flow velocities (Manners et al., 2007). Addy and Wilkinson (2019) proposed the use of reach scale 2-D morphodynamic models for predicting morphological changes (Williams et al., 2016), but these are very complex models with computational stability issues for large catchments. Morphological changes caused by leaky barriers in the river channel can alter their hydraulic feedback (Abbe & Montgomery, 1996; Manners et al., 2007; Schalko et al., 2019), so these changes would need to be measured and incorporated into the model to reflect the changing effectiveness over time.

The permeability of the barriers controls the rate at which they empty and thus influences storage availability for any subsequent events (Figures A6 and A7). Thus, a relatively permeable structure may enhance the flood reduction effect of the barriers in some circumstances. A sensitivity analysis of the permeability factor for the simulated reduction of peak flow showed only slight sensitivity at the catchment outlet. At maximum, an absolute change of 10% in the permeability factor caused a 1.3% change in the reduction in peak flow for the catchment outlet and sensitivity was reduced for less frequent flood events when water storage capacity is exceeded, and all barriers are over-topped before the peak flow takes place. Previous studies have suggested that impermeable barriers or designs that maximise the cross-sectional blockage ratio would be most effective in attenuating peak flow events, although hydraulic stresses would increase (Metcalfe et al., 2017; Muhawenimana et al., 2021). Other studies have ignored the permeability of the leaky barriers for model simplicity, assuming that the flow through the barrier is significantly lower than the flow under and over, and then setting the permeability factor to zero (Hankin et al., 2020).

Barriers in the main channel constructed early in the project proved relatively unstable resulting in the collapse of four barriers during a very large event in October 2019. The original design had a small gap at the base (9–33 cm) and was built from multiple shorter lengths of cordwood. These barriers were replaced with an improved design that increased long-term stability by using full tree trunks,

larger openings above normal winter flow levels (67–115 cm) and anchoring methods (Figure A2) which will help them to withstand hydrodynamic stress (D'Aoust & Millar, 2000; Shields & Alonso, 2012); monitoring will continue to test their integrity after flood events. This more uniform (less irregular) new design has also facilitated the estimation of the permeability factor or blockage ratio for the model (Meister et al., 2020). A few barriers particularly on the smaller tributaries showed low overall utilisation (measured by the number of days that water is stored), but these barriers may be crucial for flood attenuation during the largest flood events. Finally, Hankin et al. (2020) published advice on the best placement of barriers to maximise water storage and ensure barrier stability, suggesting areas with wider channel width and low slope. In practice, pragmatic decisions on the ground mean that leaky barriers are installed in locations that are agreed with landowners and that are easily accessible for construction machinery rather than in the optimal locations identified through modelling. This emphasises the need for strong engagement with landowners during pre-assessment studies to determine the best location to place barriers to optimise downstream flood protection whilst minimising inundation of productive cropland.

5 | CONCLUSION

Modelling studies on the effectiveness of multiple leaky barriers on reducing downstream flood risk across catchments are still limited and mainly focus on the simulation of single peak flow events. The present study used long-term field measurements and developed a modelling approach linking a physically based catchment scale model to a modified Muskingum water routing model that represents leaky barriers as permeable sluice gates. The model was set up to simulate 27 leaky barriers, calibrated and validated for a range of peak flow events over a three-year period. Overall, the modelling approach was able to capture the impact of dynamic utilisation of storage including fill up and drain down of barriers between events which is essential for quantifying the cumulative flood attenuation effect on downstream flow (Hankin et al., 2020; Muhawenimana et al., 2021). The study suggests that setting the bottom gap of leaky barriers well above winter flows and increasing the permeability of the structure will reduce channel scour and maximise storage availability between successive peak flow events.

DATA AVAILABILITY STATEMENT
The data that support the findings of this study are available from the corresponding author upon reasonable request.

ORCID
Martha L. Villamizar https://orcid.org/0000-0002-6545-3807

REFERENCES

Abbe, T. B., & Montgomery, D. R. (1996). Large woody debris jams, channel hydraulics and habitat formation in large rivers. *Regulated Rivers-Research & Management*, *12*(2–3), 201–221.

Addy, S., & Wilkinson, M. E. (2019). Representing natural and artificial in-channel large wood in numerical hydraulic and hydrological models. *Wiley Interdisciplinary Reviews: Water*, *6*(6), e1389.

Arnold, J. G., Srinivasan, R., Muttiah, R. S., & Williams, J. R. (1998). Large area hydrologic modeling and assessment - part 1: Model development. *Journal of the American Water Resources Association*, *34*(1), 73–89.

Bark, R. H., Martin-Ortega, J., & Waylen, K. A. (2021). Stakeholders' views on natural flood management: Implications for the nature-based solutions paradigm shift? *Environmental Science & Policy*, *115*, 91–98.

Burgess-Gamble, L., Ngai, R., Wilkinson, M., Nisbet, T., Pontee, N., Harvey, R., Kipling, K., Addy, S., Rose, S., Maslen, S., Jay, H., Nicholson, A., Page, T., Jonczyk, J., & Quinn, P. (2018). *Working with Natural Processes - Evidence Directory. Project SC150005*. Environment Agency: Bristol.

Cranfield University. (2014). *The soils guide*. Cranfield University. www.landis.org.uk

Daniels, M. D., & Rhoads, B. L. (2004). Spatial pattern of turbulence kinetic energy and shear stress in a meander bend with large woody debris. *Riparian Vegetation and Fluvial Geomorphology*, *8*, 87–97.

D'Aoust, S. G., & Millar, R. G. (2000). Stability of ballasted woody debris habitat structures. *Journal of Hydraulic Engineering-ASCE*, *126*(11), 810–817.

DEFRA. (2020). Countryside Stewardship grants. Department for Environment, Food and Rural Affairs. https://www.gov.uk/countryside-stewardship-grants

Environment Agency. (2015). Light detection and ranging (LIDAR) composite 2 m: UK.

Forest Research. (2016). *Slowing the flow partnership briefing: Boxing day 2015 flood event*, Slowing the flow at Pickering. Forestry Commission. https://www.forestresearch.gov.uk/research/slowing-the-flow-at-pickering/

Fry, M. J., Evans, J., Ward, H., Blake, J., Ball, L., & Doughty, L. (2014). The Provision Of Data From The COSMOS-UK Soil Moisture Monitoring Network. Paper 56, International Conference on Hydroinformatics.

Green, W. H., & Ampt, G. A. (1911). Studies on soil physics part I - the flow of air and water through soils. *Journal of Agricultural Science*, *4*, 1–24.

Hankin, B., Hewitt, I., Sander, G., Danieli, F., Formetta, G., Kamilova, A., Kretzschmar, A., Kiradjiev, K., Wong, C., Pegler, S., & Lamb, R. (2020). A risk-based network analysis of distributed in-stream leaky barriers for flood risk management. *Natural Hazards and Earth System Sciences*, *20*(10), 2567–2584.

Holdhusen, J. S., Citrini, D., Corrsin, S., Baines, W. D., Streiff, A., Henry, H. R., Albertson, M. L., Dai, Y. B., Jensen, R. A., & Rouse, H. (1950). Diffusion of submerged jets - discussion. *Transactions of the American Society of Civil Engineers*, *115*, 665–697.

Kendon, E. J., Roberts, N. M., Fowler, H. J., Roberts, M. J., Chan, S. C., & Senior, C. A. (2014). Heavier summer downpours with climate change revealed by weather forecast resolution model. *Nature Climate Change*, *4*(7), 570–576.

Leakey, S., Hewett, C. J. M., Glenis, V., & Quinn, P. F. (2020). Modelling the impact of leaky barriers with a 1D Godunov-type scheme for the shallow water equations. *Water*, *12*(2), 371.

Manga, M., & Kirchner, J. W. (2000). Stress partitioning in streams by large woody debris. *Water Resources Research*, *36*(8), 2373–2379.

Manners, R. B., Doyle, M. W., & Small, M. J. (2007). Structure and hydraulics of natural woody debris jams. *Water Resources Research*, *43*(6), w06432.

McCarthy, G. T. (1938). The unit hydrograph and flood routing. Proceedings of the North Atlantic Division Conference. United States Army Corps of Engineers, Washington, D.C., USA.

Meister, J., Fuchs, H., Beck, C., Albayrak, I., & Boes, R. M. (2020). Velocity fields at horizontal Bar racks as fish guidance structures. *Water*, *12*(1), 280.

Metcalfe, P., Beven, K., Hankin, B., & Lamb, R. (2017). A modelling framework for evaluation of the hydrological impacts of nature-based approaches to flood risk management, with application to in-channel interventions across a 29-km(2) scale catchment in the United Kingdom. *Hydrological Processes*, *31*(9), 1734–1748.

Meteoblue. (2018). *Skeffington weather station historic+ data*. Meteoblue. https://www.meteoblue.com/en/weather/archive/export/skeffington_united-kingdom_2637767

Moriasi, D. N., Arnold, J. G., Van Liew, M. W., Bingner, R. L., Harmel, R. D., & Veith, T. L. (2007). Model evaluation guidelines for systematic quantification of accuracy in watershed simulations. *Transactions of the ASABE*, *50*(3), 885–900.

Muhawenimana, V., Wilson, C. A. M. E., Nefjodova, J., & Cable, J. (2021). Flood attenuation hydraulics of channel-spanning leaky barriers. *Journal of Hydrology*, *596*, 125731.

Murphy, J. M., Sexton, D. M. H., Jenkins, G. J., Boorman, P. M., Booth, B. B. B., Brown, C. C., Clark, R. T., Collins, M., Harris, G. R., Kendon, E. J., Betts, R. A., Brown, S. J., Howard, T. P., Humphrey, K. A., McCarthy, M. P., McDonald, R. E., Stephens, A., Wallace, C., Warren, R., ... Wood, R. A. (2009). *UK climate projections science report: Climate change projections*. Exeter.

Nash, J. E., & Sutcliffe, J. V. (1970). River flow forecasting through conceptual models. Part I - a discussion of principles. *Journal of Hydrology*, *10*, 282–290.

Neitsch, S., Arnold, J., Kiniry, J., & Williams, J. (2011). Soil and water assessment tool: Theorical documentation version 2009. Texas Water Resources Institute, Collage Station, TWRI Report No. 406: Texas, USA.

Pitt, M. (2008). *The Pitt review: Learning lessons from the 2007 floods*. Cabinet Office.

Rowland, C. S., Morton, R. D., Carrasco, L., McShane, G., O'Neil, A. W., & Wood, C. M. (2017). *Land cover map 2015 (25m raster, GB)*. NERC Environmental Information Data Centre. https://doi.org/10.5285/bb15e200-9349-403c-bda9-b430093807c7

Schalko, I., Lageder, C., Schmocker, L., Weitbrecht, V., & Boes, R. M. (2019). Laboratory flume experiments on the formation of Spanwise large Wood accumulations: Part II-effect on local scour. *Water Resources Research*, *55*(6), 4871–4885.

SEPA. (2015). *Natural flood: Management handbook*. Scottish Environment Protection Agency.

Shields, F. D., & Alonso, C. V. (2012). Assessment of flow forces on large wood in rivers. *Water Resources Research*, *48*, w04516.

Smith, R. D., Sidle, R. C., Porter, P. E., & Noel, J. R. (1993). Effects of experimental removal of Woody debris on the channel morphology of a Forest. Gravel-bed stream. *Journal of Hydrology*, *152*(1–4), 153–178.

SNIFFER. (2011). Understanding the opportunities and constraints for the implementation of natural flood management features by farmers. Project FRM21. Scotland and Northern Ireland Forum for Environmental Research: Edinburgh.

Swamee, P. K. (1992). Sluice-gate discharge equations. *Journal of Irrigation and Drainage Engineering*, *118*(1), 56–60.

Thomas, H., & Nisbet, T. (2012). Modelling the hydraulic impact of reintroducing large woody debris into watercourses. *Journal of Flood Risk Management*, *5*(2), 164–174.

Viessman, W., & Lewis, G. L. (1996). *Introduction to hydrology* (4th ed.). Harper Collins College Publishers.

Villemonte, J. R. (1947). Submerged weir discharge studies. *Engineering News Record*, *139*, 866–869.

Wenzel, R., Reinhardt-Imjela, C., Schulte, A., & Bolscher, J. (2014). The potential of in-channel large woody debris in transforming discharge hydrographs in headwater areas (Ore Mountains, southeastern Germany). *Ecological Engineering*, *71*, 1–9.

Wilkinson, M. E., Addy, S., Quinn, P. F., & Stutter, M. (2019). Natural flood management: Small-scale progress and larger-scale challenges. *Scottish Geographical Journal*, *135*(1–2), 23–32.

Williams, P., Biggs, J., Stoate, C., Szczur, J., Brown, C., & Bonney, S. (2020). Nature based measures increase freshwater biodiversity in agricultural catchments. *Biological Conservation*, *244*, 108515.

Williams, R. D., Measures, R., Hicks, D. M., & Brasington, J. (2016). Assessment of a numerical model to reproduce event-scale erosion and deposition distributions in a braided river. *Water Resources Research*, *52*(8), 6621–6642.

Wingfield, T., Macdonald, N., Peters, K., Spees, J., & Potter, K. (2019). Natural flood management: Beyond the evidence debate. *Area*, *51*(4), 743–751.

Wohl, E. (2013). Floodplains and wood. *Earth-Science Reviews*, *123*, 194–212.

SUPPORTING INFORMATION

Additional supporting information can be found online in the Supporting Information section at the end of this article.

How to cite this article: Villamizar, M. L., Stoate, C., Biggs, J., Szczur, J., Williams, P., & Brown, C. D. (2024). A model for quantifying the effectiveness of leaky barriers as a flood mitigation intervention in an agricultural landscape. *River Research and Applications*, 1–14. https://doi.org/10.1002/rra.4241